

Cooling performance analysis of Magnetic Nanofluids comparing with transformer oil and air

¹**PRASANT KUMAR SWAIN**, *Gandhi Institute of Excellent Technocrats, Bhubaneswar, India*

²**PRIYANSU SWAIN**, *Gopal Krishna College of Engineering and Technology, Koraput, Odisha, India*

Magnetic-thermal-fluidic analysis were conducted to assess the cooling performance of magnetic nanofluids by comparing the performance with that of transformer oil and air using the fully coupled finite element method (FEM) considering the magnetoconvection phenomena. Magnetic nanofluids (MNFs) have been studied extensively for bio- and nanotechnology applications. In particular, some studies reported that the MNF has good characteristics for thermal management and electric insulation in experiments. With this motivation, this study focused on the cooling performance of MNFs including the experimental and numerical approaches. Until now, research on the cooling effect of MNF has focused mainly on heat propagation without any real magnetic system, in which the magnetic force plays a key role in driving fluidic flow. This flow driven by the magnetic force density was related to the magnetoconvection effect. To analyze this effect quantitatively, a coupled analysis technique should be developed using the magnetic-thermal-fluidic equations. To validate the cooling performance of MNFs numerically, the numerical results were verified by a comparison with those from the experimental tests in the air, transformer oil, and MNF. After confirming the numerical setup, some experiments were conducted with a vertical solenoid coil immersed in a MNF with different volume fractions of magnetic nanoparticles. The temperature at the inside part of the coil decreased dramatically by approximately 5 °C in the 7 vol. % MNF compared to the transformer oil. These temperatures were also predicted well using the proposed numerical setup.

Index Terms—Cooling performance, Kelvin force density, magnetic nanofluids, magnetoconvection, multiphysics analysis, transient hot wire system.

I.

INTRODUCTION

RECENTLY, magnetic nanofluids (MNF) has been studied extensively for bio- and nanotechnology applications with numerical and experimental approaches [1]–[6]. In particular, some studies have reported enhanced cooling performance and dielectric breakdown strength in electromagnetic systems, such as power transformer [7], [8]. As a coolant material, MNFs can enhance the convection phenomena with an applied magnetic field, called magnetoconvection [9]. Because magnetization is inversely proportional to temperature, the cooler magnetic fluid is pushed toward the direction of the gradient of the magnetic field intensity and replaces the hotter magnetic fluid.

In previous studies, a coupled magnetic-thermal-fluidic analysis technique was constructed to analyze the cooling effect of MNF [10]. In that case, however, the simulation was limited to an artificial numerical model because there was no precise measuring system for evaluating the thermal conductivity of MNF. In addition, in that method, the numerical results were not confirmed with the experimental data and only the magnetoconvection effect depending on temperature in a magnetic system was proposed.

To analyze this effect quantitatively, the coupled analysis technique should be developed by combining the magnetic-thermal-fluidic equations and precise material property values. Measuring the thermal conductivity is quite difficult because nanofluids contain nanoparticles in their fluids. To resolve this difficulty, this study adopted the transient hot wire system, which has been used widely to measure the thermal conductivity of nanofluids [11]. From this experiment, the thermal conductivity was approximately 0.154 W/mK under 42 °C. In the current experimental setup, the temperature rise was in this range. Hence, this study could be conducted using this value. In addition, the proposed numerical setup uses the conjugate heat transfer (CHT) technique, which is an advanced algorithm for interpolating the temperature at the interface between the solid conductor and MNF. This model was solved using the COMSOL Multiphysics software applications and finite element method (FEM) to determine if the cooling performance of MNF is better than that of transformer oil or air due to the magnetoconvection effect driven by the additional magnetic force density.

Finally, to confirm the numerical setup, a straight wire immersed in the MNF was constructed and the temperature rise was compared. Subsequently, the temperature rise was predicted for a solenoid coil and the results were compared with the experimental data.

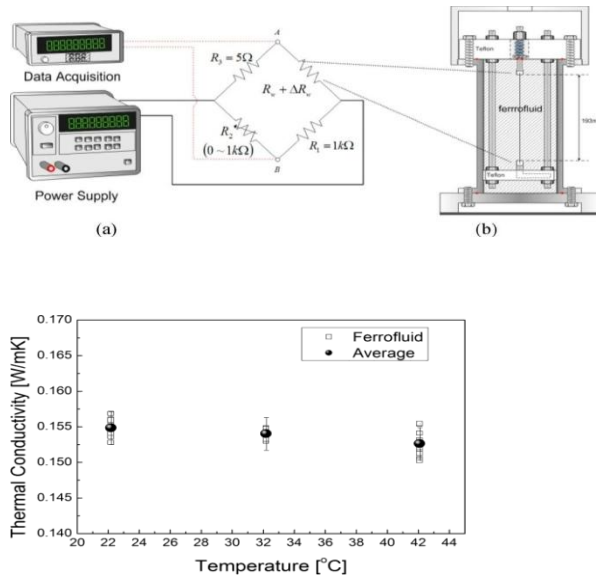


Fig. 1. Schematic diagram of a transient hot wire apparatus. Note that the ferrofluid denotes the MNF. (a) Wheatstone bridge. (b) Cylinder.

II. THERMAL CONDUCTIVITY OF MAGNETIC NANOFUID BY USING THE TRANSIENT HOT WIRE SYSTEM

The transient hot wire system is used widely for determining the thermal conductivity of the fluids accurately [11]. Fig. 1 shows the transient hot wire system used in this study. As shown in Fig. 1(a), the Wheatstone bridge consists of two fixed resistances, R_1 and R_3 , a variable resistor, R_2 , and R_w , a resistance of hot Pt wire included in the transient hot wire system. In particular, the Pt wire was insulated electrically by a Teflon coating and had resistance of 8.9 Ω at 0 $^{\circ}\text{C}$ measured in-house. The temperature coefficient resistivity of the wire was 0.00392 ($1/^{\circ}\text{C}$). The wire was immersed into a cylinder filled with the MNF, as shown in Fig. 1(b), to measure the thermal conductivity of MNF.

The transient hot wire system explains how to measure the thermal conductivity as follows: a long and thin wire suspended vertically in a liquid with thermal conductivity was heated at time, $t \geq t_0$, with a constant heat flux per unit time per unit length. The wire loses heat radially into the liquid through conduction alone. More heat is conducted if the thermal conductivity of the liquid is larger. Therefore, the slope of the temperature of the wire as a function of time was relatively small. On the other hand, if the thermal conductivity is smaller, the slope of the wire is relatively larger. These phenomena have been well modeled theoretically with the assumption that the heat is transferred from the center of the wire to infinite circumstances with the radial directions as follows:

$$k = \frac{q}{4\pi(T_2 - T_1)} \ln\left(\frac{t_2}{t_1}\right) \quad (1)$$

where k and q are the thermal conductivity and applied power per unit length of the wire, respectively, and \ln is the temperature rise of the wire between times t_1 and t_2 .

To confirm the accuracy and reliability of this experimental system, the thermal conductivity of distilled water was measured before obtaining that of MNF, and the uncertainty of the thermal conductivity measurements was within 1.5%.

The thermal conductivity of MNF was measured at 22 $^{\circ}\text{C}$, 32 $^{\circ}\text{C}$ and 42 $^{\circ}\text{C}$, respectively, as shown in Fig. 2. The thermal conductivity of MNF showed no temperature dependence from

22 $^{\circ}\text{C}$ to 42 $^{\circ}\text{C}$ and the thermal conductivity of MNF had a constant value of approximately 0.154 W/mK.

Fig. 2. Thermal conductivity of MNF. Note that the ferrofluid denotes the MNF.

III. GOVERNING EQUATIONS FOR MAGNETIC-THERMAL-FLUIDIC ANALYSIS

The governing equations for magnetic-thermal-fluidic analysis were composed of the Ampere's law, the energy balance equation, and Navier-Stoke's equation as follows:

$$\nabla \times \mathbf{H} = \mathbf{J} \quad (2)$$

$$\frac{\partial T}{\partial t} + \mathbf{v} \cdot \nabla T = \frac{1}{\rho_l c_v} (k_T \nabla^2 T + \mathbf{E} \cdot \mathbf{J}) \quad (3)$$

$$\rho_l \frac{\partial \mathbf{v}}{\partial t} - \nabla \cdot [\eta (\nabla \mathbf{v} + (\nabla \mathbf{v})^T)] + \rho_l (\mathbf{v} \cdot \nabla) \mathbf{v} + \nabla p = \mathbf{F} \quad (4)$$

$$\nabla \cdot (\rho_l \mathbf{v}) = 0 \quad (5)$$

where \mathbf{H} is the magnetic field intensity, \mathbf{J} is the current density, \mathbf{v} is the fluidic velocity, ρ_l and c_v are the mass density and specific heat capacity, respectively, k_T is the thermal conductivity, η is the dynamic viscosity, p is the pressure, and \mathbf{F} is the body force density.

IV. BUOYANCY AND MAGNETIC BODY FORCE DENSITIES To consider the body force effects, the Kelvin force for the magnetic field gradient and the Boussinesq buoyant force for temperature gradient were included as follows [12]:

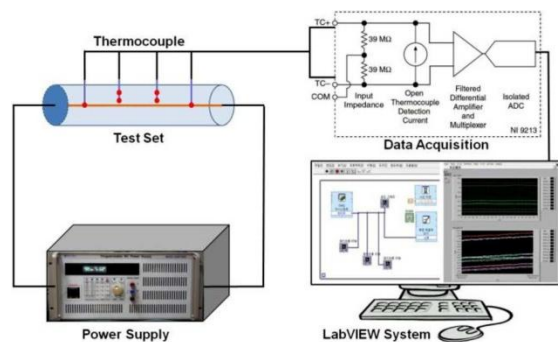
$$\mathbf{F} = \mu_0 \mathbf{M} \cdot \nabla \mathbf{H} + (-\rho_l \beta (T - T_{\text{ref}}) \mathbf{g}) \quad (6)$$

where \mathbf{M} denotes the magnetization, β is the thermal expansion coefficient, T_{ref} is the buoyancy reference temperature, and \mathbf{g} is the acceleration due to gravity. The Kelvin force density as a function of temperature, volume fraction and nanoparticle size was used as the driving source for the magnetoconvection phenomena in the MNF.

V. EXPERIMENTAL AND NUMERICAL RESULTS

A. Verification Model With Experiments

To confirm the numerical technique, first, a simple experimental setup was constructed to measure the temperature, as shown in Fig. 3. This system was composed of a DC power supply, test set with a straight wire of 1 m, NI 9213 for data



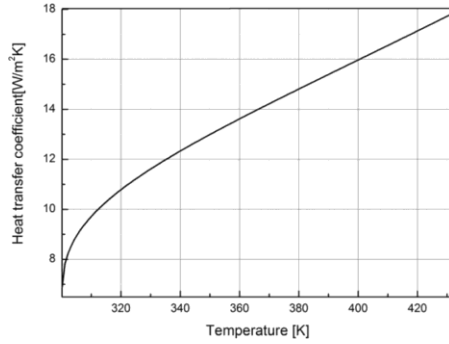


Fig. 3. Schematic diagram of a straight wire system with a data acquisition setup to measure the temperatures. The data acquisition setup was composed of the LabVIEW and NI 9213 from National Instruments Inc.

TABLE I
HIGHEST TEMPERATURES AT THE CONDUCTOR

Material Type	Temperature Rise, T (°C)	
Input Current: 6 A	Numerical Analysis	Experiments
Air	36.95	35.16
Transformer Oil	28.77	28.61
Magnetic Nanofluid (7%)	28.14	28.17

*) Highest temperatures were obtained at the center of conductor and these data corresponded to the temperature distribution as shown in Fig. 6.

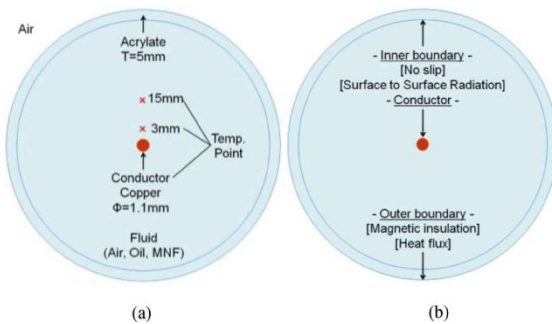


Fig. 4. Numerical analysis model in 2-D XY geometry and boundary setup for a straight wire system. (a) Numerical analysis model setting. (b) Boundary setting.

acquisition from National Instruments Inc., and the LabVIEW software for recording the temperature. The temperatures at a steady state of 6 A with air, transformer oil, and MNF of 7 vol. % were 35.16 C, 28.61 C and 28.17 C, respectively, as listed in Table I. A large difference was observed between air and the fluidic media, but the temperature of air and MNF was similar. Because the gradient of the magnetic field was too small, the magnetoconvection effect was also too weak to generate fluidic flow. Therefore, this model is good for validating the numerical setup.

B. Verification of Numerical Results

Fig. 4 shows the numerical analysis model and boundary setup for a straight wire system, as shown in Fig. 3. The CHT solver was used for a more accurate simulation at the interface between the solid and fluidic region, and the effective heat

Fig. 5. Effective heat transfer coefficient as a function of temperature when the emissivity is 0.94 [12].

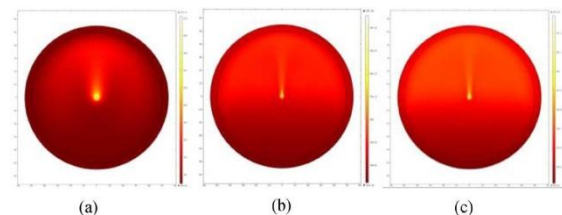


Fig. 6. Numerical results of the temperature distributions in each medium. The conjugate heat transfer solver was used to interpolate the temperature distribution at the interface of the solid and fluid region. (a) Air. (b) Transformer oil. (c) Magnetic nanofluid.

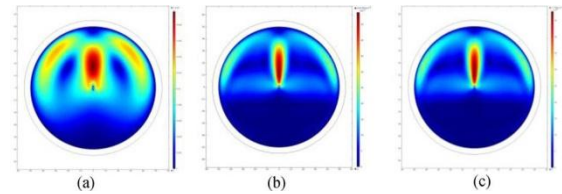


Fig. 7. Numerical results of velocity field in each medium. (a) Air. (b) Transformer oil. (c) Magnetic nanofluid.

transfer coefficient used to exclude the outside air region for saving computing time, as shown in Fig. 5 [12]. Figs. 6 and 7 show the distributions of temperature and velocity fields with each medium, such as air, transformer oil, and MNF. As shown in Table I, the temperatures from the numerical simulation were in good agreement with those from the experiments. Therefore, the numerical setup is sufficiently reliable for this problem. Although the Kelvin force was small, the net force pushes the fluid upward and accelerates the fluidic flow, resulting in enhanced cooling performance, as shown in Fig. 8.

C. Application to Solenoid Coil and Magnetic-Thermal-Fluidic Analysis

To show the magnetoconvection effect actively, the solenoid coil with a radius of 8.75 mm and 40 turns was fabricated, as shown in Fig. 9. In this model, the Kelvin force density was much stronger than the straight wire model, and a magnetoconvection effect will occur actively inside the solenoid. Figs. 10 and 11 show the temperature distributions from the experimental results. The temperature of the MNF was much lower than that of the transformer oil, and the temperature

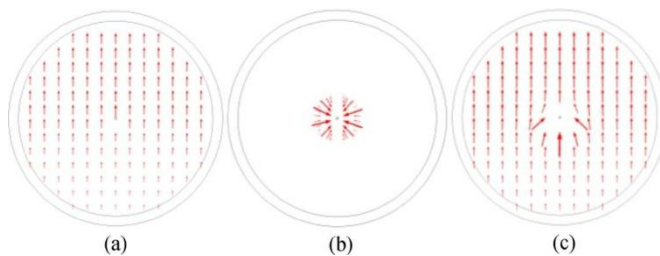


Fig. 8. Force density distributions. The total force represents the summing force of buoyant and Kelvin forces. The maximum vectors were different from one another and the vectors were magnified in each case. (a) Buoyant force. (b) Kelvin force. (c) Total force.

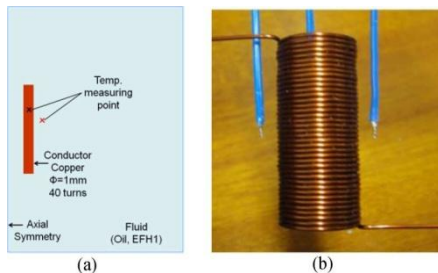


Fig. 9. Solenoid model for testing the cooling performance of MNF. (a) 2-D experimental model. (a) Analysis model. (b) Real model.

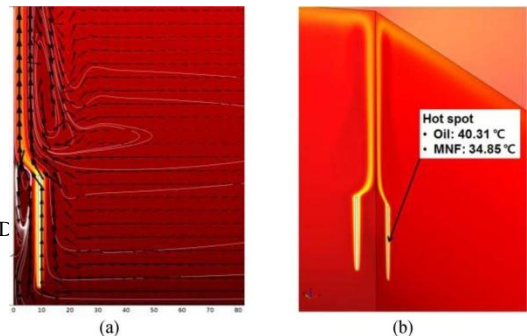


Fig. 12. Numerical results for inductor model. The temperatures were almost the same as those from the experiments as shown in Fig. 10. (a) Flow vectors and streamline. (b) Temperature distribution.

VI.

CONCLUSION

A fully-coupled magnetic-thermal-fluidic analysis technique was developed successfully and verified using the experimental setup. The magnetoconvection effect was the dominant mechanism for cooling in magnetic systems with MNF. The cooling characteristics and the proposed numerical setup will be used for the thermal management of the transformer.

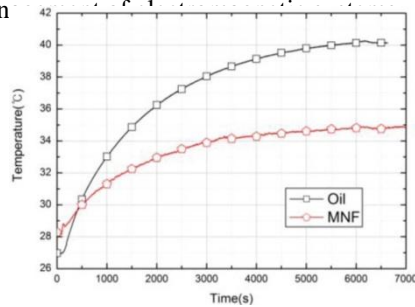


Fig. 10. Experimentally determined temperature rise at conductor with different media, conventional transformer oil and MNF of 7% in volume fraction.

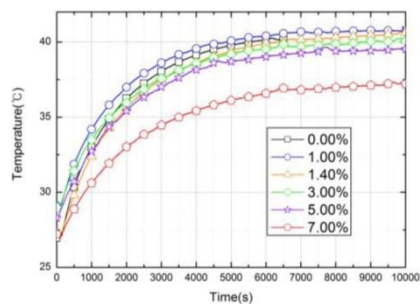


Fig. 11. Experimentally determined temperature rise as a function of the volume fraction from 0 to 7%. Note that the temperature increased slightly with 1% MNF.

decreased with increasing volume fraction. Fig. 12 shows the numerical results for flow and temperature. The temperature of the hot spot was predicted well using the proposed numerical setup.

REFERENCES

- [1] G. Yoshikawa, K. Hirata, F. Miyasaka, and Y. Okaue, "Numerical analysis of transitional behavior of ferrofluid employing MPS method and FEM," *IEEE Trans. Magn.*, vol. 47, no. 5, pp. 1370–1373, May 2011.
- [2] M. Balli, C. Mahmed, P. Bonhote, and O. Sari, "On the magnetic forces in magnetic cooling machines: Numerical calculations and experimental investigations," *IEEE Trans. Magn.*, vol. 47, no. 10, pp. 3383–3386, Oct. 2011.
- [3] Y. Okaue, G. Yoshikawa, F. Miyasaka, and K. Hirata, "Study on analysis method for ferrofluid," *IEEE Trans. Magn.*, vol. 46, no. 8, pp. 2799–2802, Aug. 2010.
- [4] H. S. Choi, Y. S. Kim, K. T. Kim, and I. H. Park, "Simulation of hydrostatic equilibrium of ferrofluid subject to magneto-static field," *IEEE Trans. Magn.*, vol. 44, no. 6, pp. 818–821, Jun. 2008.
- [5] R. M. Erb and B. B. Yellen, "Model of detecting nonmagnetic cavities in ferrofluid for biological sensing applications," *IEEE Trans. Magn.*, vol. 42, no. 10, pp. 3554–3556, Oct. 2006.
- [6] A. Nethe, T. Scholz, H.-D. Stahlmann, and M. Filtz, "Ferrofluids in electric motors—A numerical process model," *IEEE Trans. Magn.*, vol. 38, no. 2, pp. 1177–1180, Feb. 2002.
- [7] V. Segal and K. Raj, "An investigation of power transformer cooling with magnetic fluid," in *Proc. Symp. Recent Trends Sci. Technol. Magn. Fluids*, India, Oct. 1997.
- [8] V. Segal, A. Hjortsberg, A. Rabinovich, D. Nattrass, and K. Raj, "AC (60 Hz) and impulse breakdown strength of a colloidal fluid based on transformer oil and magnetite nanoparticles," in *Proc. 1998 IEEE Int. Symp. Electr. Insulation*, 1998, pp. 619–622.
- [9] S. M. Snyder, T. Cader, and B. A. Finlayson, "Finite element model of magnetoconvection of a ferrofluid," *J. Magnet. Magn. Mater.*, vol. 262, pp. 269–279, 2003.
- [10] S.-H. Lee and Y.-S. Kim, "Finite element analysis for cooling effect of magnetic fluid with alternating magnetic field," *J. Appl. Phys.*, vol. 105, p. 07B510, 2009.
- [11] J.-H. Lee, K. S. Hwang, S. P. Jang, B. H. Lee, J. H. Kim, S. U. S. Choi, and C. J. Choi, "Effective viscosities and thermal conductivities of aqueous nanofluids containing low volume concentrations of Al₂O₃ nanoparticles," *Int. J. Heat Mass Transfer*, vol. 51, pp. 2651–2656, 2008.
- [12] Y. A. Cengel and R. H. Turner, *Fundamental of Thermal-Fluid Sciences*, 2nd ed. New York, NY, USA: McGraw-Hill, 2005.